Metasurface-based planar microlenses integrated on back-side illuminated CMOS pixels 1 st

Martin Lepers, Alain Ostrovsky, Patrice Genevet, Stéphane Lanteri, Jérôme Vaillant

Metasurface-based planar microlenses integrated on back-side illuminated CMOS pixels

1st Martin Lepers
STMicroelectronics
CRHEA
Grenoble, France
martin.lepers@st.com

2nd Alain Ostrovsky
STMicroelectronics
Grenoble, France
alain.ostrovsky@st.com

3rd Patrice Genevet
Univ. de Côte d'Azur
CRHEA
Valbonne, France
patrice.genevet@crhea.cnrs.fr

4th Stéphane Lanteri
Univ. de Côte d'Azur
Inria, CNRS, LJAD
Sophia Antipolis, France
stephane.lanteri@inria.fr

5th Jérôme Vaillant
Univ. Grenoble Alpes
CEA-Leti
Grenoble, France
jerome.vaillant@cea.fr

***Abstract*—Metasurface based microlenses (or metalenses) are planar microlenses which could be an alternative to replace refractive microlenses made of resist on image sensor. This paper aims at exploring through simulation the integration of metalenses on CMOS pixel array. Theses simulations precede metalenses implementation on STMicroelectronics 2.8, 4 and 8 µm pixels with updated fabrication process involving immersion photolithography. Emphasis is given on improving metalenses performances with consideration to fabrication capacities available.**

***Index Terms*—CMOS, BSI, metasurface, microlens, metalens, immersion photolithography**

I. Introduction

Based on prior work on FSI planar microlenses to improve the sensitivity of Single Photon Avalanche Diode SPAD [1], [2] further studies are being conducted to adapt the technology on CMOS back-side illuminated pixel[1].

Metasurfaces are nanostructured surfaces capable of manipulating light at a sub-wavelength scale to achieve a macroscopic optical function [3]–[6]. The microlenses designs discussed in this article are based on metasurfaces encoded with a phase profile allowing the concentration of light at a given focal length. They are composed of sub-wavelength cylindrical pillars of high-index material embedded in a low-index material substrate. By modulating the pillars diameter it is possible to induce localized phase-shift which could then be spatially distributed to replicate the phase profile of a lens.

II. Fabrication Process

Demonstrators on industrial CMOS image sensors are currently under fabrication and characterization will be available in the second half of 2023. This generation of metalenses is fabricated with an updated version of the previous generation process [2]: 193 nm immersion photolithography and improved OPC (Optical Proximity Correction) are used to achieve more aggressive design (smaller minimum pillar diameter) and better control of pillar size. As of today, the fabrication process started and metrology tools such as SEM are used to control the fabrication (see Fig. 1).

[1]The design wavelength for the microlenses based on metasurface is 940 nm

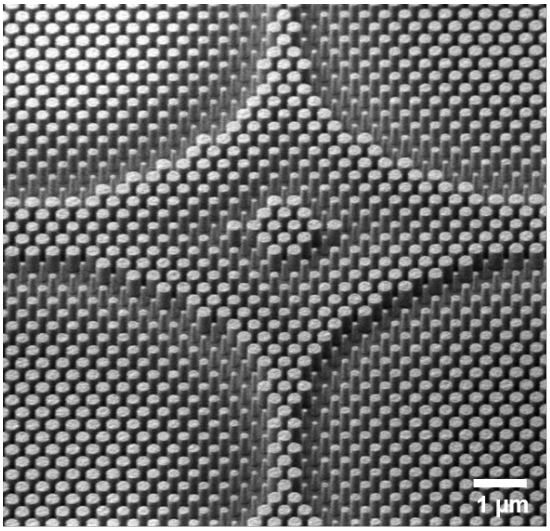

Fig. 1: Tilted SEM view of a 2×2 metalenses array made with immersion photolithography tool.

III. Simulation

In the following section we examine different design approaches for metalenses. At first we will discuss the metalenses geometry with consideration to their focalization properties and then present recent work about phase profile engineering.

A. Simulation workflow

The metalenses discussed in this paper follow the design method described in [1], [2]. The phase profile of a perfect lens is sampled with unitary pillars (meta-atoms or nanopillars) of various diameters inducing local phase-shift. Those meta-atoms are arranged in 2D space to reproduce the targeted phase profile. The set of parameters (pitch, height, radius) defining the structure of the pillars is referred as "library" (see Fig. 2) and is obtained through FDTD[2] (Lumerical FDTD) and RCWA[3] (Reticolo) simulations.

To evaluate the performance of a design, the optical stack is simplified to its essentials features and simulated with

[2]Finite Difference Time Domain
[3]Rigorous Couple Wave Analysis

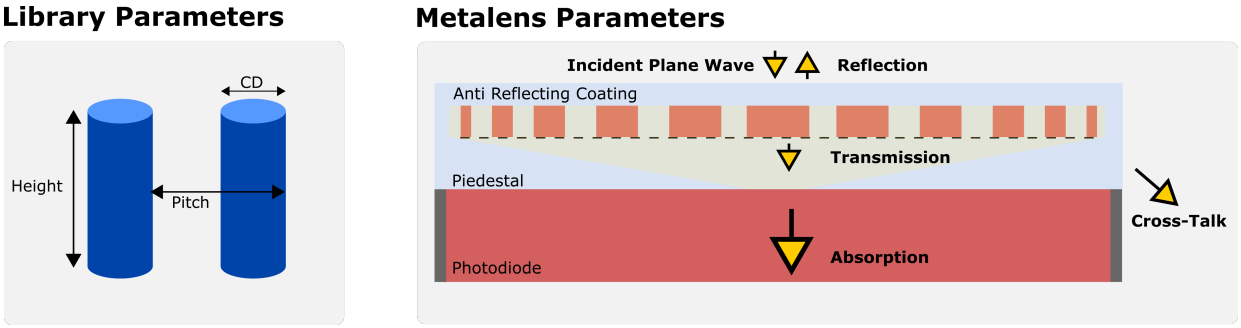

Fig. 2: Schematic of library parameters (left) and description of a metalens integrated on a simplified pixel (right).

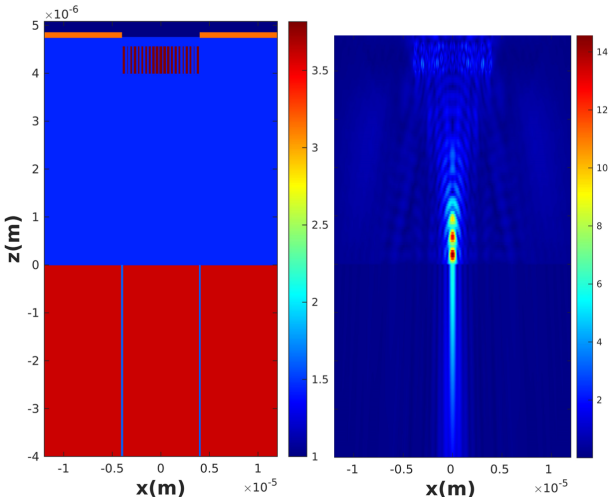

Fig. 3: (Left) Refractive index visualization of the simulation (Right) Electric Field (V/m) in the simulation. We simulate a square metalens of 8 µm width with a focal length of 4 µm on top of a 3×3 pixels (red) array isolated from each other by isolation trench (vertical blue lines). The lens is embedded in silicon oxyde (blue) and tungsten shielding (orange) is added to estimate cross-talk.

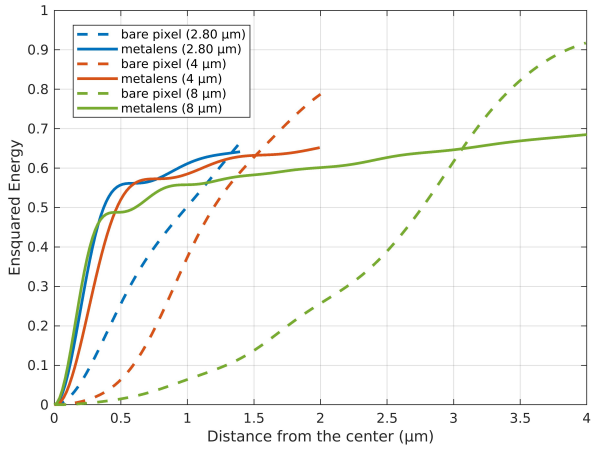

Fig. 4: Ensquared energy comparison between a pixel with metalens (solid line) and a pixel without metalens (dashed line).

Lumerical-FDTD (see Fig. 3). The studied metalens is embedded in silicon dioxide and lays on a pedestal which height is a design parameter. Another layer of oxide is added on top of the stack to reduce reflection. The photodiode is surrounded by isolation trenches which goal is to reduce cross-talk. In the simulation a shielding[4] (tungsten) is added to evaluate the light loss due to diffraction outside the targeted pixel which is also referred as optical cross-talk. For each simulation the aperture size in the shielding is equal to the width of the metalens.

B. Microlens geometry

Simulations are performed on metalenses that have the same size as the pixels they are placed on, which is the most commonly used configuration for imaging devices. Focus is given on the amount of light transmitted to the photodiode as we consider total absorption in the silicon and zero cross-talk due to the isolation trenches.

We calculate the metalenses ensquared energy (see Fig. 4) in the focal plane to assess their focusing efficiency. The calculation involves integrating the Poynting vector flux over an increasing square surface area. We observe an intensity distribution in the focal plane following the profil of an altered Airy disk. We consider the focusing efficiency as the ratio between intensity inside a square of width equals to the diameter of the Airy spot first dark ring (which we estimated to be 0.5 µm) and the intensity collected by the total surface area. For pixel size of 2.80, 4 and 8 µm with a fixed focal length of 4 µm we find the associated focusing efficiency of 87 %, 79% and 71%. As metasurface allows arbitrary manipulation of phase through the variation of pillar diameter, metalenses enables focalization properties out of reach for melted refractive microlenses limited by the fabrication process. Low numerical-aperture and off-axis [2] metalenses have been simulated on pixels array of 2×2, 3×3 and 4×4 pixels to assess their performances (see Fig. 5 to Fig. 7).

Improvement on the library [2] (denoted library 1, pitch=370 nm, height=350 nm) used to design metalenses on FSI SPAD was also studied through multiple simulations at the nanopillar and at the metalens scale. A more compact library (denoted library 2, pitch=300 nm, height=750 nm) demonstrated better performances than the previously used set of pillars. This library have been selected after running simulations of nanopillars through most of the parameter space considering the updated fabrication process. It has been

[4]It is important to note that shielding will not be present on the fabricated structure but the aperture does create additional diffraction in the simulation

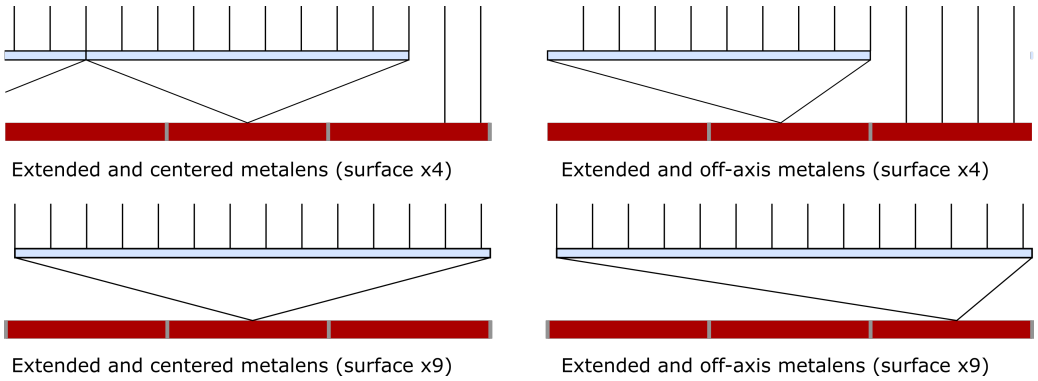

Fig. 5: Schematic of an extanded metalens and an off-axis metalens positioned over an array of 2×2 and 3×3 pixels.

selected for its transmission and focalization performances given the considered size and focal length of the metalens. As the surface of the lens expands, we observe continuous increase of the intensity transmitted to the photodiode with a maximum gain of 9.5 for a metalens with a surface area 16 times larger than the pixel. For off-axis metalenses the simulations show a maximal gain of 6.85 for the same surface extension. For each design variation, the library 2 increases the transmission to the targeted photodiode in comparison to library 1. A maximum gain of 1.31 is achieved between the two centered metalenses with a surface area 16 times the area of the photodiode.

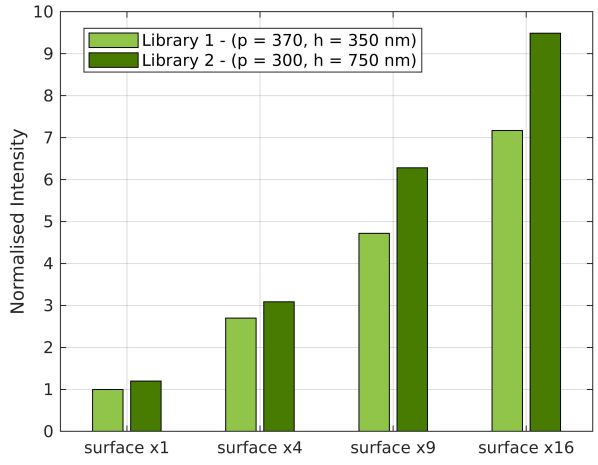

Fig. 6: Centered metalens simulated transmission for various footprint surface. The surface of the metalenses increases from left to right and both library 1 (light green) and library 2 (dark green) are used. Focal length is 4 µm.

Simulations show an overall performances increase with the compact library with lower reflection and cross-talk than the one used previously. It may be explained by a better sampling of the phase profile allowed by the smaller pitch.

C. Phase profile investigation

Most metalenses designs in literature are based on a hyperbolic phase profile (1), in this section, we evaluate the use of a quadratic phase profile (2). Quadratic phase profile translates a linear phase (which corresponds to a plane wave with oblique incidence) into spatial shift and so the effect of a non-zero incidence would be a spatial translation of the focal spot whereas it would spread with a hyperbolic phase profile.

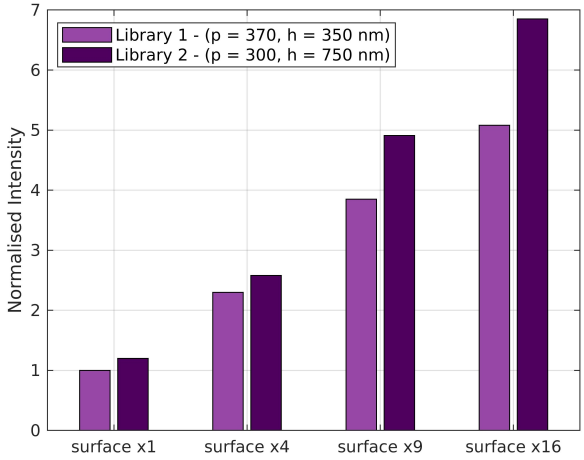

Fig. 7: Off-Axis metalens simulated transmission for various footprint surface. The surface of the metalenses increases from left to right and both library 1 (light purple) and library 2 (dark purple) are used. Focal length is 4 µm.

$$\phi_{hyp}(r) = -k_0 n(\sqrt{f^2 + r^2} - f) \tag{1}$$

$$\phi_{quad} = \frac{-k_0 n}{2f} r^2 \tag{2}$$

with k_0 the wavevector, n the index of the substrate, f the encoded focal length and r the radial coordinate on metasurface plane. Following the work on wide FOV metalenses [7], we implement on the pixel stack previously described a hyperbolic metalens and a quadratic metalens with a focal length f = 4 µm and a size of D = 4 µm. As the incident angle varies it is expected to observe a lower expansion of the focal spot for the quadratic lens in comparison of the hyperbolic lens and therefore to achieve a better angular tolerance.

Simulations show that the FWHM (Full Width at Half Maximum) of both metalenses focal spots increases with incident angle (see Fig. 8). However as the incident angle increases, the quadratic phase profile shows a better resilience to maintain the expansion of the focal spot with a 40 nm difference for a angle of $45°$. As expected the quadratic metalens presents a bigger focal spot at normal incidence

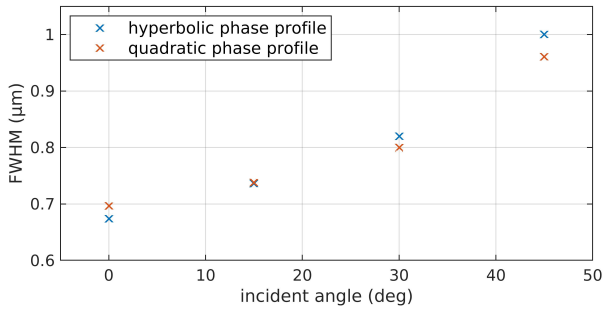

Fig. 8: FWHM variation of the focal spot with incident angle for a lens designed with a hyperbolic phase profile (blue) and with a quadratic phase profile (orange).

as quadratic phase profile introduces spherical aberrations. These simulations results suggest that the phase profile may be optimized at the metalens scale to design angle resilient metalenses for imaging system.

D. Phase profile encoding

Different approachs can be used to design phase optics based on metasurfaces. Previously we referred to the look-up table method to create libraries which consist in running simulation of unitary pillar, extract the induced phase-shift, and use them as a database to sample the targeted phase profile. Research on "CMOS-compatible all-dielectric metalens" [8] presents a different design approach based on an effective-index n_{eff} modulation and Maxwell-Garnett mixing rule. We propose here a performance comparison between those designs of metalenses. Pillar pitch and height is fixed at p=370 nm and h=550 nm but for the effective-index metalens, pillar diameter D is calculated analytically with the equation (3) and (4).

$$D(r) = \sqrt{\frac{4}{\pi} p^2 F(r)} \tag{3}$$

$$F(r) = \frac{n_{eff}^2(r) - n_0^2}{n_{eff}^2(r) + n_0^2} \frac{n_p^2 + n_0^2}{n_p^2 - n_0^2} \tag{4}$$

with $F(r)$ a filling fraction calculated using the Maxwell-Garnett mixing rules, n_p the index of the aSi pillars and n_0 the index of the substrate.

We observe an overall equivalent transmission between the effective-index based and the hyperbolic metalens (See Fig. 9). However the difference is more visible for the reflection and the cross-talk. It can be explained by the final aspect of these metalenses and particularly their pillar distribution. The effective-index based metalens has less pillar due to phase-shift value out of reach with the existing index contrast. With less pillar on its trajectory the reflection decreases and the transmission increases but we observe also an increase of the cross-talk due a more restricted phase range.

Conclusion

We studied metalenses integrated on BSI CMOS pixel able to focus light and increase the amount of light reaching the photodiode. We demonstrated overall performance

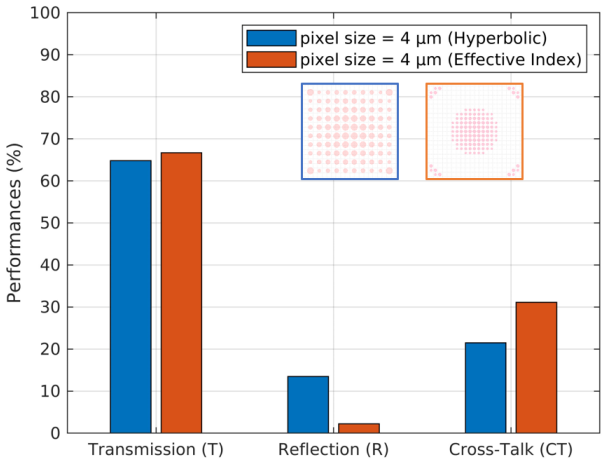

Fig. 9: Performance comparison between a hyperbolic (blue) and an effective-index based metalens (orange).

improvement using a compact library involving an higher height/diameter ratio nanopillars. Performance evaluation were also conducted to compare hyperbolic and quadratic phase profile. Finally design of a metalens based on Maxwell-Garnett analytic calculation of effective index have been performed. Demonstrators on CMOS image sensor are currently under fabrication and characterization will be presented in a future paper. The use of optimization algorithm was not considered in the presented design and it may be explored for next generation metalenses.

Acknowledgements

We thank all the people who work on the wafers in the cleanrooms both at STMicroelectronics and at the CEA Leti. M. Lepers also would like to thanks both teams of INRIA and CRHEA for their advice and guidance and Raphal Mulin for his support on the effective-index metalens simulation.

References

[1] L.Dilhan, J.Vaillant, A.Ostrovsky, L.Masarotto, C.Pichard, et R.Paquet, "Planar microlenses for near infrared CMOS image sensors", *Electron. Imaging, In vol.2020, n°7, p.144-1-144-7, janv.2020.*

[2] L.Dilhan *et al.*, "Planar microlenses applied to SPAD pixels", In: *IISW proceedings, 2021.*

[3] Steven J. Byrnes, Alan Lenef, Francesco Aieta, and Federico Capasso, "Designing large, high-efficiency, high-numerical-aperture, transmissive meta-lenses for visible light," In *Opt. Express 24, 5110-5124 (2016).*

[4] P.Lalanne, P.Chavel, "Metalenses at visible wavelengths: Past, present, perspectives.", In *Laser Photonics Rev. 2017, 11, 1600295.*

[5] P. Genevet, F. Capasso, F. Aieta, M. Khorasaninejad, and R. Devlin, "Recent advances in planar optics: from plasmonic to dielectric meta-surfaces", In *Optica 4, 139-152 (2017).*

[6] H.Benisty, J.Greffet, P.Lalanne, "Introduction to Nanophotonics", *Oxford Graduate Texts.*

[7] Augusto Martins *et al.*, "On Metalenses with Arbitrarily Wide Field of View", In: *ACS Photonics 2022 7 (8), 2073-2079.*

[8] E.Mikheeva *et al.*, "CMOS-compatible all-dielectric metalens for improving pixel photodetector arrays", In *APL Photonics 5, 116105 (2020).*